Nonlinear Dynamics and Applications. Vol. 30 (2024) 383 - 389

Analysis of K_S^0 production in SPD at NICA

Natalia Rogacheva, on behalf of the SPD Collaboration*
Joint Institute for Nuclear Research (JINR)
Joliot-Curie st, 6, Dubna, Moscow Region, Russia

In this work, the analysis of the inclusive K_S^0 production and transverse single spin asymmetry (TSSA) in proton-proton interactions with a center of mass energy of 27 GeV is performed for the upcoming Spin Physics Detector (SPD) experiment at the NICA collider (Nuclotron-based Ion Collider Facility). The simulation is done using the SpdRoot framework. Results of K_S^0 reconstruction are shown as functions of multiple kinematic variables. The K_S reconstruction efficiency is split into separate contributing factors and the estimates of the feed-down fractions are provided.

PACS numbers: 13.25.Es
Keywords: SPD, NICA, strange particle, K-Short meson.

1. Introduction

The puzzle of the origin of the proton and deuteron spin has been an active area of both experimental and theoretical research for the last thirty years. Despite considerable efforts, a complete understanding of this structure remains an challenging. Measurements related to the studies of the spin structure of proton and deuteron, as well as other spin-related phenomena, are parts of the research program at the future Spin Physics Detector (SPD) to be constructed at the Nuclotron-based Ion Collider fAcility (NICA) in the Joint Institute for Nuclear Research. The details of the SPD experimental setup are described in the Conceptual Design Report [1].

While the main objective of the SPD experiment is comprehensive study of the unpolarized and polarized gluon content of the nucleon, the experiment can also provide valuable information on the spin-dependent quark structure of proton and (the spin-dependent QCD) dynamics via measuring transverse single-spin asymmetries (TSSA), sometimes termed the analyzing power (A_N), in hadron production. For collision energies where the quark model is applicable, these asymmetries are related to transverse momentum dependent parton distributions (TMD PDFs like transversity and Sivers functions) and Collins fragmentation function. Of particular interest are the spin asymmetries observed in K-meson production, primarily because of the involvement of the s-quark in the final state which emerges from the 'sea'. Measurements of SSA for the K_S^0 mesons have been performed only for polarized proton beams with the momentum of 13.3 GeV/c and 18.5 GeV/c on the Be target in the central region[2, 3]. In Fig. 1 the analyzing power is shown as a function of Feynman-x (x_F). The analyzing power for K_S^0 displayed a significant negative asymmetry of approximately 0.1 for $x_F < 0.2$ with the asymmetry increasing with x_F.

*E-mail: rogacheva@jinr.ru

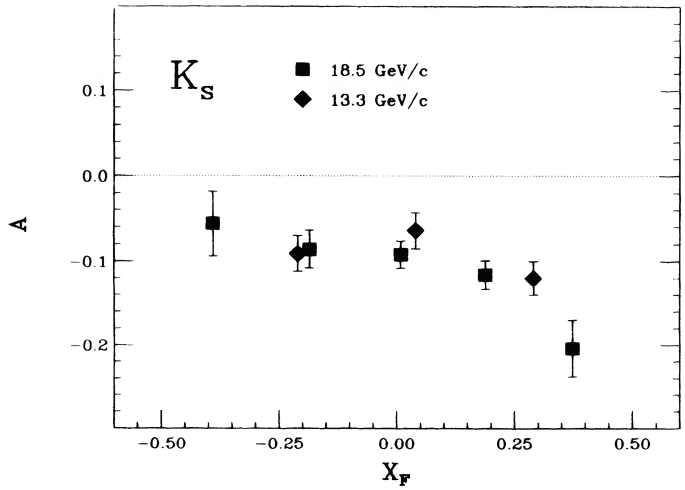

Figure 1: A_N results for K_S^0 as a function of x_F for the two beam energies.

To determine the feasibility of measuring the TSSA of the inclusive K_S^0 production at the SPD, first the K_S^0 reconstruction efficiency is evaluated and then statistical errors for SSA are estimated for 1 year of data taking at the maximum collision energy.

2. Analysis

The SpdRoot framework, derived from the FairRoot software [4], was used for the detector simulation and event reconstruction. Proton-proton collisions were simulated at a center-of-mass energy $\sqrt{s} = 27$ GeV using the Pythia 8 generator [5] configured for the simulation of minimum bias events. The transportation of particles through the detector and magnetic field of the SPD setup was provided by Geant4 [6]. Track fitting was performed using the GenFit toolkit [7]. KFparticle package [8] was used to reconstruct the secondary vertex from the $K_s^0 \to \pi^+\pi^-$ decay (the branching ratio is 69.20%). The generated data sample consists of 4 million events, which corresponds to approximately 1 second of data taking at the SPD.

The selection of the K_S^0 was based on the search for secondary vertices. The K_S^0 decay pion candidates were required to be well-fitted and have $\chi^2_{track}/N_{df} < 6$, where χ^2_{track} and N_{df} are χ^2 and the number of degrees of freedom in the track fit. To suppress the combinatorial background, the tracks that could be extrapolated back to the primary vertex ($\chi^2_{extrap} < 10$) were excluded. Each possible pair of such tracks with opposite charges was considered a K_S^0 candidate. The track pairs were required to have a common vertex (the vertex fit satisfies $\chi^2_{SV} < 2$). The reconstructed K_S^0 should originate from the primary vertex ($\chi^2_{K_S \to PV} < 2$) and the collinearity angle, θ_{coll}, between the reconstructed K_S^0 momentum and the direction between the reconstructed primary and secondary vertices was constrained to $\theta_{coll} < 0.03$ rad. Only K_S^0 candidates with decay length above 0.7 cm were accepted. Without the aid of particle identification, there are kinematic regions populated by both $\Lambda^0(\bar{\Lambda}^0)$ and K_S^0 decays. Depending upon the type of analysis, the kinematic overlap region may introduce important biases. In this analysis, the kinematic overlap region was achieved by a cut on the "helicity angle": $|\cos(\theta^*)| < 0.8$, where θ^* was defined as the angle between the π^+ momentum vector in the K_S^0 rest frame and the boost vector from the laboratory system to the K_S^0 rest frame. The resulting suppression of Λ and $\bar{\Lambda}$ contamination is shown in Fig. 2.

The invariant mass of the K_S^0 candidates after the imposed cuts is shown in Fig. 3.

The distribution was fitted with the sum of a double Gaussian for the K^0_S signal and a second-order polynomial for the background. In total, about 96 thousand events of K^0_S were selected in the analysis.

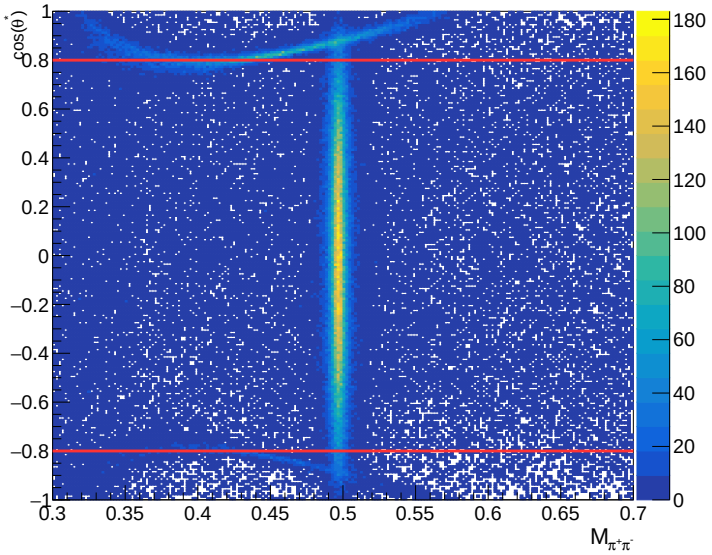

Figure 2: A scatter plot of the helicity angle of the π^+ candidate versus the $\pi^+\pi^-$ candidate pair invariant mass in the data. The vertical K^0_S band is clearly visible. The lower and upper curved bands are due to the Λ and $\bar{\Lambda}$ (respectively) in the sample.

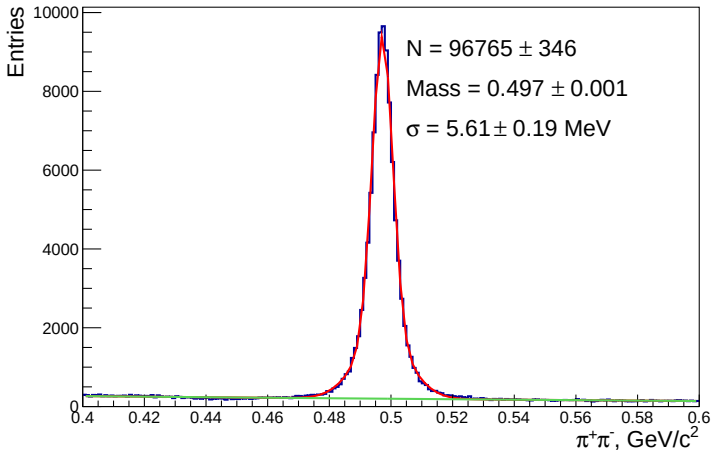

Figure 3: Invariant mass distribution of $K^0_S \to \pi^+\pi^-$ after applying selection cuts for the full analysis sample.

Kinematic distributions of momentum versus polar angle ($N(p, \theta)$), Feynman-x variable versus transverse momentum ($N(x_F, p_T)$), and rapidity versus transverse momentum ($N(y, p_T)$) for the generated and reconstructed K^0_S events are shown in Fig. 4. In the reconstructed events, there are regions (shown by red areas) in which the influence of the beam pipe at small or large θ angles for a high momentum is observed. Impact of this effect can also be observed on x_F and y distributions.

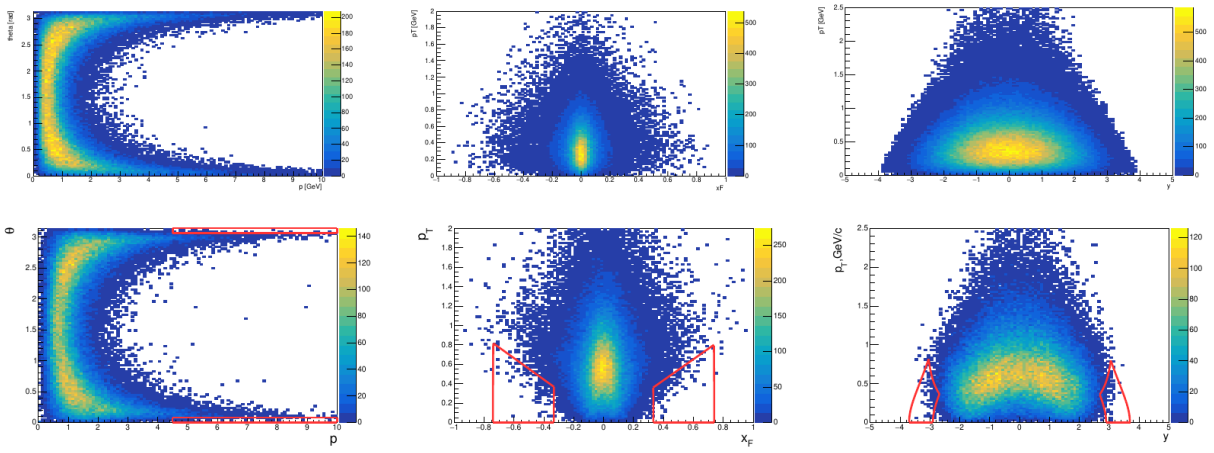

Figure 4: Kinematic distributions $(N(p,\theta))$, $(N(x_F,p_T)$ and $(N(y,p_T))$ of K^0_S for generated (top row) and reconstructed (bottom row) events.

The distribution of selected K^0_S candidates in the (p,θ)-space is shown in Fig. 5. The choice of the binning scheme is driven by the available statistics to retain similar number of kaons in every bin. For this analysis, 40 non-equidistant bins with 4 equal θ bins and 10 non-equidistant θ-dependent p bins for each were used. A fit of the invariant mass distribution was performed in each of these (p,θ) bins.

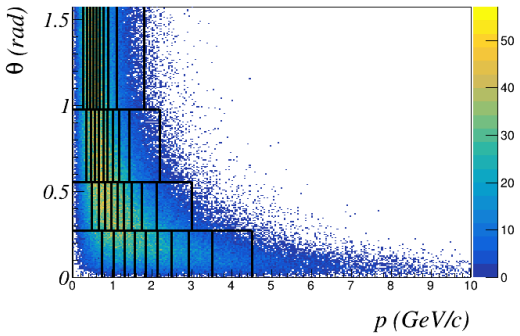

Figure 5: The (p,θ)-space of K^0_S in the SPD acceptance region is shown. The binning used in the analysis is indicated by the black boxes.

The coefficient C, that relates the number of the directly produced K_S mesons at the primary interaction point $(N^{gen}_{K_S})$ and the total number of reconstructed mesons $(N^{rec}_{K_S})$ was factorized into 10 contributions as follows:

$$C = \frac{N^{rec}_{K_S}}{N^{gen}_{K_S}} = C0 \cdot C00 \cdot C1 \cdot C2 \cdot C3 \cdot C4 \cdot C5 \cdot C6 \cdot C7 \cdot C8. \quad (1)$$

Table 1 lists all coefficients and their definitions. Factorized coefficients are shown as functions of the momentum for fixed θ intervals in Fig. 6. The coefficients $C1 - C8$ describe different contributions to the selection efficiency. Additionally, we separate the direct K^0_S production from decays of K^* and other particles via $C0$, and K^0_S produced in the primary interaction from those generated in the detector material via $C00$.

Table 1: Short description of factorization coefficients in equation 1.

Coefficient	Formula	Short description
C0	$\frac{N(K^0_{true} inPV)}{N(K^0_{gen})}$	Feed down in primary vertices (K^0_S from direct production)
C00	$\frac{N(K^0_{true}(all))}{N(K^0_{true} inPV)}$	Feed down correction outside primary vertices (K^0_S produced in the detector material)
C1	$\frac{N(3hits)}{N(K^0_{true}(all))}$	Geometrical acceptance
C2	$\frac{N(\chi^2/NDF_{tr1,2}<6)}{N(3hits)}$	Well-fitted track candidates
C3	$\frac{N(\chi^2_{V0}<2.0)}{N(\chi^2/NDF_{tr1,2}<6)}$	Fit of the two-track vertex
C4	$\frac{N(\chi^2_{tr1,2} toPV>10)}{N(\chi^2_{V0}<2.0)}$	Extrapolation of the K_S vertex to the primary vertex
C5	$\frac{N(well-convergency)}{N(\chi^2_{tr1,2} toPV>10)}$	Well-converged fit for tracks
C6	$\frac{N(\theta_{coll}<0.03)}{N(well-converged)}$	Collinearity angle for K_S decay
C7	$\frac{N(Dist>0.7)}{N(\theta_{coll}<0.03)}$	K_S decay length
C8	$\frac{N(\lvert cos\theta^*\rvert \leqslant 0.8)}{N(Dist>0.7)}$	Helicity angle for π^+ from K_S decay

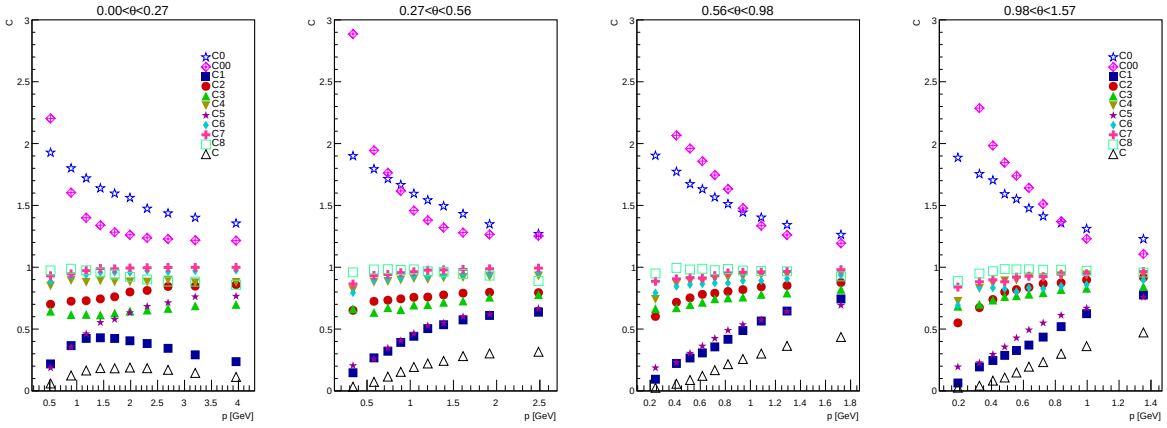

Figure 6: Factorized contributions to the K^0_S reconstruction efficiency and feed-down fractions as function of the momentum for fixed θ intervals.

The major impact to the selection efficiency come from $C1$, $C2$, and $C5$, the other coefficients contribute about 5 or 10 %. The K^0_S reconstruction efficiency depends on p and θ and varies from 30% at low θ to 10% at high θ. In the first θ bin (small angle), impact of the beam pipe can be observed, where typically one of the pions from K^0_S decay is lost resulting in reduced reconstructed efficiency.

3. Estimation of the Statistical Uncertainty of TSSA

At the time of this study, no event generators were available to simulate events with TSSA for inclusive meson production. Nevertheless, it is possible to make an estimate of the statistical uncertainty for A_N. It is known that for the least-squares method and the linear model (e.g., fitting the histogram with a sum of the constant term plus the cosine modulation), the uncertainty of each contribution depends on the shapes of the individual contributions and the overall uncertainty of the binned data. In our case, for $A_N \ll 1$, the estimates for the statistical uncertainties can be made for the $A_N = 0$ case. Under the same assumption, the following rough approximation can be used.

The TSSA of K_s^0 production is analyzed as the functions of x_F in the range $-0.40 < x_F < 0.40$ with the bin size of 0.05, assuming all events were recorded by the online filter. The yield $N(K_s^0(\phi))$ and its uncertainty are evaluated in 8 equal ϕ-bins ($\phi \in [-\pi, \pi]$) as follows. In each bin, the invariant mass of $\pi^+\pi^-$ was fitted with a second order polynomial function for the background and a normalized Gaussian distribution representing the signal peak. The number of events and its uncertainty are taken from the fit scaled to the expected statistics per one year of data taking. These 8 values with their uncertainties are then fitted with the function

$$N(K_s^0(\phi)) = A(1 + P_B A_N \cdot \cos\phi) \tag{2}$$

using the χ^2-minimization technique, provided by the MINUIT package of ROOT. Here $P_B \sim 0.7$ accounts for the expected beam polarization. Statistical uncertainty of A_N in x_F bins for 1 year (10^7 sec) of SPD data taking are shown in Fig. 7. One concludes that precision of such measurement at SPD will be dominated by the systematic uncertainties.

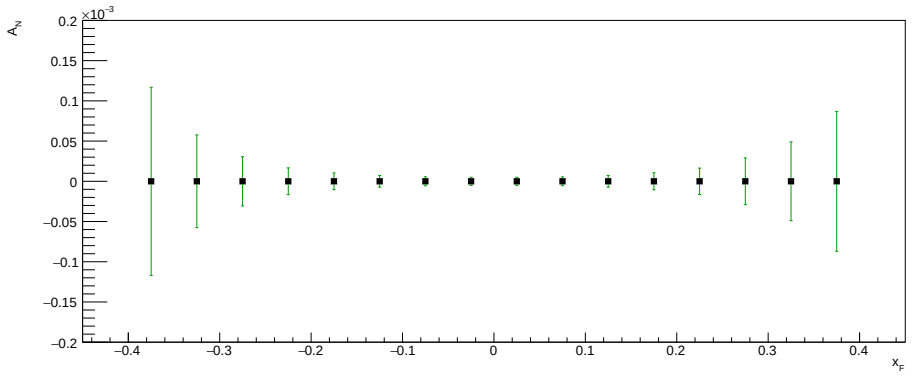

Figure 7: Statistical A_N error in x_F intervals.

4. Conclusion

Reconstruction efficiency of K_S^0 meson production and estimates of the statistical uncertainties of its transverse single spin asymmetries have been presented here. For this purpose, an analysis of proton-proton collisions at the center of mass energy 27 GeV were performed at the generator level and full event reconstruction was done at detector level. As demonstrated in the work, K_S^0 reconstruction efficiency depends on momentum and polar angle and varies from 30% at low θ to 10% at high θ.

References

[1] Technical Design Report of the Spin Physics Detector, Version 1.0 Apr 12, (2024)–https://spd.jinr.ru/physics-detector/Technical Design Report of the Spin Physics Detector.pdf

[2] B.E. Bonner et al., Spin-parameter measurements in Λ and K_S^0 production, Phys.Rev.D 38 (1988) 729.

[3] B.E. Bonner et al., Analyzing power of inclusive production of π^-, π^+ and K_S^0 by polarized protons at 13.3 and 18.5 GeV/c, Phys.Rev.D 41 (1990) 13.

[4] M. Al-Turany, D. Bertini, R. Karabowicz, D. Kresan, P. Malzacher, T. Stockmanns, and F. Uhlig. The FairRoot framework. J. Phys. Conf. Ser., 396:022001, 2012.

[5] Torbjorn Sjostrand, Stefan Ask, Jesper R. Christiansen, Richard Corke, Nishita Desai, Philip Ilten, Stephen Mrenna, Stefan Prestel, Christine O. Rasmussen, and Peter Z. Skands. An Introduction to PYTHIA 8.2. Comput. Phys. Commun., 191:159-177, 2015, 1410.3012.

[6] J. Allison et al. Recent developments in Geant4. Nucl. Instrum. Meth. A, 835:186-225, 2016.

[7] J. Rauch, T. Schluter, GENFIT - a Generic Track-Fitting Toolkit, J. Phys. Conf. Ser. 608 (1) (2015) 012042.

[8] S. Gorbunov, I. Kisel, Reconstruction of decayed particles based on the Kalman filter, Tech. Rep. CBM-SOFT-note-2007-003, CBM Collaboration (2007).